# A contact detection algorithm for superellipsoids based on the common-normal concept

C. Wellmann * , C. Lillie and P. Wriggers

*Institute of Mechanics and Computational Mechanics*
*Leibniz University of Hannover*
*Appelstr. 9A, Hannover, Germany*
*E-mail:*
*wellmann@ibnm.uni-hannover.de*
*lillie@ibnm.uni-hannover.de*
*wriggers@ibnm.uni-hannover.de*

* Corresponding author.

*Preprint submitted to Elsevier* *11 May 2007*

# A contact detection algorithm for superellipsoids based on the common-normal concept

**Paper type**
Research paper
**Purpose**
Introduction of an efficient contact detection algorithm for smooth convex particles.
**Design/methodology/approach**
The contact points of adjacent particles are defined according to the common normal concept. The problem of contact detection is formulated as two-dimensional unconstrained optimization problem that is solved by a combination of NEWTON's method and a LEVENBERG-MARQUARDT method.
**Findings**
The contact detection algorithm is efficient in terms of the number of iterations required to reach a high accuracy. In the case of non-penetrating particles a penetration can be ruled out in the course of the iterative solution before convergence is reached.
**Research limitations**
The contact detection algorithm is only applicable to smooth convex particles, where an explicit relation between the surface points and the surface normals is available.
**Originality/value**
By a new kind of formulation the problem of contact detection can be reduced to a two-dimensional unconstrained optimization problem. Furthermore this formulation enables a very fast contact exclusion in the case of non-penetrating particles.
**Keywords**
contact detection algorithm, superellipsoid, DEM

## Introduction

Contact detection of moving rigid bodies is an important problem in various fields like Discrete Element Methods (DEMs), Computer Vision, Robotics, etc. When dealing with numerous bodies the process of contact detection is split into two phases: In the first phase the number of potential contact pairs is reduced with the help of bounding boxes and spatial sorting algorithms. In the second phase a detailed contact check is performed for the resulting potential contact pairs. An overview of methods for both parts of the process is given by Lin and Gottschalk (1998) and Vemuri et al. (1998). Obviously, the particle type is crucial for the kind of algorithm that might be applied for the detailed contact check. Particle types can be divided into discrete types

consisting of a number of vertices with a corresponding connectivity and continuous types which can be described with the help of implicit or explicit continuous functions. These particle types are further subdivided into convex and non-convex types. Regarding DEMs continuous particles have the advantage of an uniquely defined normal at every surface point, which is favorable for the calculation of contact forces. The simplest kind of continuous particles are spheres for which contact detection is trivial. More sophisticated particle types which were successfully used in DEMs are e.g. ellipsoids (Ting et al., 1995; Lin and Ng, 1995; Ouadfel and Rothenburg, 1999), the four-arc ellipsoid approximation (Potapov and Campbell, 1998; Wang et al., 1999; Kuhn, 2003; Johnson et al., 2004), and superellipsoids (Barr, 1981; Williams and Pentland, 1992; Cleary et al., 1997). In contrast to the four-arc ellipsoid approximation ellipsoids and superellipsoids have a continuous curvature, which facilitates the use of a more sophisticated, HERTZIAN-type contact law.
This paper introduces an efficient algorithm for the second phase of contact detection, that is applicable to any kind of continuous convex particles, that offer an explicit relationship between the surface points and surface normals. The algorithm is described and tested using superellipsoid particles, which offer the greatest variety of shapes among the continuous particles quoted above. It is build as an iterative search for the contact direction, which is the direction parallel to the surface normals at the contact points. In this process the algorithm exploits the convex shape of the particles by searching for a separating plane, such that each particle lies in a different half-space of the plane. Hence, in the case of non-penetrating particles it is possible to rule out a penetration before final convergence is reached which reduces the computational effort significantly.
The paper is organized as follows: First, a short introduction of superellipsoids and their important properties regarding the contact detection algorithm is given. Next, the problem of contact detection is formulated as a two-dimensional unconstrained optimization problem in terms of the contact direction. The application of a combined NEWTON and LEVENBERG-MARQUARDT method then leads to the contact detection algorithm. This is followed by an extensive validation of the algorithm and the conclusion.

## Superellipsoid

Superellipsoid particles like introduced by Barr (1981) are used, whose definition differs slightly from those used by Williams and Pentland (1992) and Cleary et al. (1997). According to Barr a superellipsoid is described by the so-called inside-outside function

$$F(\boldsymbol{x}) = \left( \left| \frac{x_1}{r_1} \right|^{\frac{2}{\epsilon_1}} + \left| \frac{x_2}{r_2} \right|^{\frac{2}{\epsilon_1}} \right)^{\frac{\epsilon_1}{\epsilon_2}} + \left| \frac{x_3}{r_3} \right|^{\frac{2}{\epsilon_2}} . \tag{1}$$

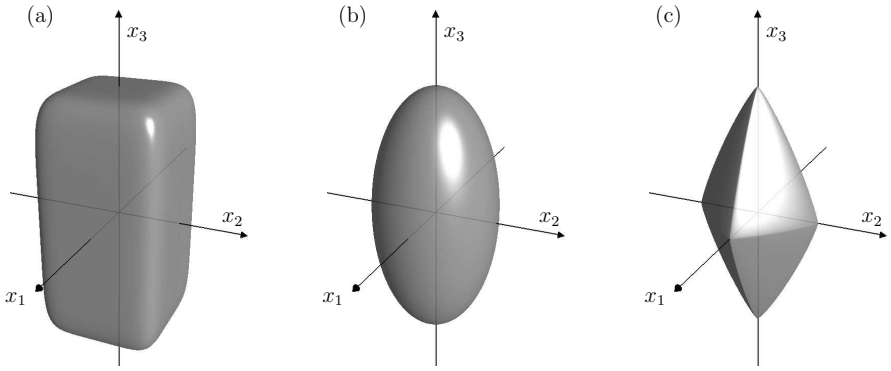


Fig. 1. Superellipsoids with $r_1 = r_2 = r_3/2$ and $\epsilon_i = 0.3$ (a), $\epsilon_i = 1$ (b) and $\epsilon_i = 1.7$ (c).

Every point $\boldsymbol{x}$ with $F(\boldsymbol{x}) \leq 1$ belongs to the superellipsoid and every point $\boldsymbol{x}$ with $F(\boldsymbol{x}) = 1$ lies on its surface. The radius parameters $r_i$ specify the dimensions of the superellipsoid. The exponents $\epsilon_1$ and $\epsilon_2$ control the squareness of the superellipsoid in the $x_1$,$x_2$ plane and $x_3$ direction respectively. Here $\epsilon_i \in (0, 2)$ is assumed which leads to a convex body. Note, that $\epsilon_i \to 0$ yields a cuboid and $\epsilon_i \to 2$ yields an octahedron, compare Fig. 1. Furthermore, it is possible to describe the surface of the superellipsoid in terms of surface parameters $\phi_i$ through

$$\boldsymbol{x}(\phi_1, \phi_2) = \begin{bmatrix} \operatorname{sgn}(\cos\phi_1)\ r_1\, |\cos\phi_1|^{\epsilon_1}\, |\cos\phi_2|^{\epsilon_2} \\ \operatorname{sgn}(\sin\phi_1)\ r_2\, |\sin\phi_1|^{\epsilon_1}\, |\cos\phi_2|^{\epsilon_2} \\ \operatorname{sgn}(\sin\phi_2)\ r_3\, |\sin\phi_2|^{\epsilon_2} \end{bmatrix}, \quad \begin{aligned} -\pi &\leq \phi_1 < \pi \\ -\tfrac{\pi}{2} &\leq \phi_2 \leq \tfrac{\pi}{2}\,. \end{aligned} \tag{2}$$

Regarding the contact detection algorithm a favorable property of superellipsoids is that the surface normals are easily described in terms of the surface parameters by another superellipsoid equation

$$\boldsymbol{n}(\phi_1, \phi_2) = \begin{bmatrix} \operatorname{sgn}(\cos\phi_1)\ (1/r_1)\ |\cos\phi_1|^{2-\epsilon_1}\, |\cos\phi_2|^{2-\epsilon_2} \\ \operatorname{sgn}(\sin\phi_1)\ (1/r_2)\ |\sin\phi_1|^{2-\epsilon_1}\, |\cos\phi_2|^{2-\epsilon_2} \\ \operatorname{sgn}(\sin\phi_2)\ (1/r_3)\ |\sin\phi_2|^{2-\epsilon_2} \end{bmatrix}. \tag{3}$$

Hence, there is a smooth invertible mapping between the two-dimensional space of surface parameters and the three-dimensional space of normalized normal vectors. The surface parameters are expressed in terms of the normal

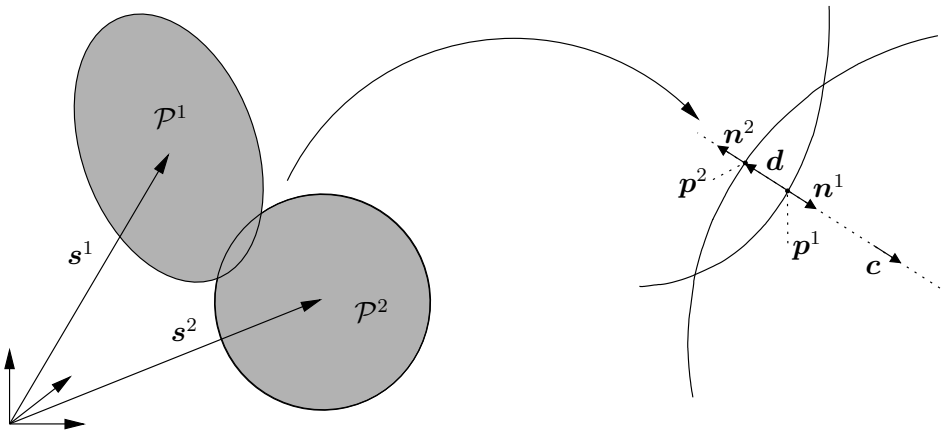


Fig. 2. Two adjacent particles $\mathcal{P}^1$ and $\mathcal{P}^2$ with contact points $\boldsymbol{p}^1$ and $\boldsymbol{p}^2$, normal vectors $\boldsymbol{n}^1$ and $\boldsymbol{n}^2$, distance vector $\boldsymbol{d}$ and contact direction $\boldsymbol{c}$.

components $n_i$ by

$$\begin{aligned}
\phi_1 &= \tan^{-1}\left(s_1\,|r_1\,n_1|^{\delta_1},\ s_2\,|r_2\,n_2|^{\delta_1}\right) \\
\phi_2 &= \begin{cases} \tan^{-1}\left(|r_1\,n_1|^{\delta_2},\ s_3\,|\,(r_3\,n_3\,|\cos\phi_1|^{2-\epsilon_1}\,)\,|^{\delta_2}\right) & \text{if } |r_1\,n_1| > |r_2\,n_2| \\ \tan^{-1}\left(|r_2\,n_2|^{\delta_2},\ s_3\,|\,(r_3\,n_3\,|\sin\phi_1|^{2-\epsilon_1}\,)\,|^{\delta_2}\right) & \text{else} \end{cases} \\
&\text{with} \quad \delta_i = 1/\,(2-\epsilon_i)\,, \quad s_i = \operatorname{sgn}(n_i)\ .
\end{aligned} \tag{4}$$

Herein $\tan^{-1}(x,y)$ is the arc tangent of $y/x$, taking into account which quadrant the point $(x,y)$ is in.

## Problem formulation

In DEMs a contact detection algorithm has to check if two adjacent particles $\mathcal{P}^1$ and $\mathcal{P}^2$ inter-penetrate and calculate the set of quantities used for contact force generation. For most of the contact formulations used in DEMs contact points $\boldsymbol{p}^1$ and $\boldsymbol{p}^2$, a penetration distance $d = \|\boldsymbol{d}\| = \|\boldsymbol{p}^2 - \boldsymbol{p}^1\|$ and a contact direction $\boldsymbol{c}$ belong to this set, compare Fig. 2. Regarding contact force generation a definition of the contact points based on the common-normal concept is favorable, see (Johnson, 1985). Accordingly the contact points are defined as those points that have minimum distance and fulfill the following set of conditions

$$\begin{aligned}
\boldsymbol{n}^1 &= \mu^2\,\boldsymbol{c} \\
\boldsymbol{n}^2 &= -\nu^2\,\boldsymbol{c} \\
\boldsymbol{d}\times\boldsymbol{c} &= \boldsymbol{0}\,.
\end{aligned} \tag{5}$$

Herein $\boldsymbol{n}^1$ and $\boldsymbol{n}^2$ are the outward surface normals at $\boldsymbol{p}^1$ and $\boldsymbol{p}^2$ and $\mu$ and $\nu$ are arbitrary real numbers. Conditions $(5)_1$ and $(5)_2$ assure that the normal

vectors are anti-parallel and $(5)_3$ assures that the vector connecting $\boldsymbol{p}^1$ and $\boldsymbol{p}^2$ is parallel to the contact direction $\boldsymbol{c}$.
Since the normal vectors can be expressed in terms of the surface points coordinates, (5) can be formulated as a set of nonlinear equations in these coordinates by elimination of $\boldsymbol{c}$. This set of nonlinear equations can be used to determine $\boldsymbol{p}^1$ and $\boldsymbol{p}^2$, whereat attention has to be paid to multiple solutions, because the minimum distance condition is neglected. This approach was used successfully in combination with ellipsoids (Lin and Ng, 1995) and superellipsoids (Cleary et al., 1997). Other approaches for the determination of contact points that only approximately fulfill (5) are methods based on geometric potential functions (Ting et al., 1993; Lin and Ng, 1995; Tijskens et al., 2004) and the discrete function representation (DFR) approach (Williams and O'Connor, 1995; Hogue, 1998). For the first kind of methods the contact point definition is based on the geometric potential function of the particles which for superellipsoids is the inside-outside function (1). Lin and Ng (1995) e.g. define the contact points as those points which minimize the geometric potential function of the other particle. For a small penetration these methods yield contact points close to that defined by (5). In the second approach each particle surface is discretized by a number of points. Contact detection is then done by checking these points for inclusion in the adjacent particle. The DFR approach allows for a wider range of particle shapes which do not have to be convex. It's accuracy regarding (5) and it's performance depend on the number of points used for the surface discretization.
The crucial point of the approach introduced here is that the problem of contact detection is formulated in terms of the contact direction $\boldsymbol{c}$. For this purpose the contact direction is parameterized by two angles $\alpha_1$ and $\alpha_2$ through

$$\begin{aligned} &\boldsymbol{c}\left(\alpha_1,\alpha_2\right) = \cos\alpha_1\,\cos\alpha_2\,\boldsymbol{e}_1 + \sin\alpha_1\,\cos\alpha_2\,\boldsymbol{e}_2 + \sin\alpha_2\,\boldsymbol{e}_3 \\ &\text{with} \quad \boldsymbol{e}_1 = \left(\boldsymbol{s}^2 - \boldsymbol{s}^1\right)/\|\boldsymbol{s}^2 - \boldsymbol{s}^1\| \quad \text{and} \quad \boldsymbol{e}_i \cdot \boldsymbol{e}_j = \delta_{ij}\,. \end{aligned} \tag{6}$$

Herein $(\boldsymbol{e}_1, \boldsymbol{e}_2, \boldsymbol{e}_3)$ are the unit base vectors of a right-handed Cartesian coordinate system with $\boldsymbol{e}_1$ pointing in the direction from the first particle center to the second particle center. In the next step the surface points $\boldsymbol{p}^1$ and $\boldsymbol{p}^2$ have to be determined in terms of $\alpha_1$ and $\alpha_2$ so that $(5)_1$ and $(5)_2$ are fulfilled. Therefore, the contact direction $\boldsymbol{c}\left(\alpha_1,\alpha_2\right)$ has to be transformed into the local coordinate systems of both particles. For each particle the transformation between the components of local $(\tilde{\bullet})$ and global position and direction vectors is given with the particle center vector $\boldsymbol{s}$ and it's rotation tensor $\boldsymbol{T}$ by

$$\begin{aligned} x_i &= T_{ij}\,\tilde{x}_j + s_i \\ d_i &= T_{ij}\,\tilde{d}_j\,. \end{aligned} \tag{7}$$

Next, the surface parameters of the points where the normal is parallel and anti-parallel to $\boldsymbol{c}\left(\alpha_1,\alpha_2\right)$ respectively can be determined using (4). Finally $\boldsymbol{p}^1\left(\alpha_1,\alpha_2\right)$ and $\boldsymbol{p}^2\left(\alpha_1,\alpha_2\right)$ can be derived from the surface parameters with

the help of (2) and (7). Consequently, the distance vector can be expressed in terms of the contact direction angles

$$\boldsymbol{d}\left(\alpha_1, \alpha_2\right) = \boldsymbol{p}^2\left(\alpha_1, \alpha_2\right) - \boldsymbol{p}^1\left(\alpha_1, \alpha_2\right) . \tag{8}$$

Hence, the problem of contact detection can be formulated as optimization problem in terms of the contact direction angles through

$$\min_{\alpha_1, \alpha_2} \; f\left(\alpha_1, \alpha_2\right) = \left\| \boldsymbol{d}\left(\alpha_1, \alpha_2\right) \right\|^2 . \tag{9}$$

Note, that condition $(5)_1$ and $(5)_2$ are always fulfilled because of the construction of the surface points. Furthermore, it can be shown that condition $(5)_3$ is fulfilled at the global minimum of (9) if the penetration distance is small compared to the particle sizes and compared to the minimum radius of curvature of the particle surfaces. Hence, the global minimum of (9) yields the contact direction of (5) from which the other quantities necessary for contact force generation can be derived.

### Contact detection algorithm

For an implementation of a contact detection algorithm any unconstrained optimization algorithm might be applied to problem (9). Here a combination of Newton's method and a Levenberg-Marquardt method is used. Hence, the first and second derivatives of $f$ with respect to the contact direction angles have to be determined

$$f_i = 2\left(\boldsymbol{d} \cdot \boldsymbol{d}_i\right), \quad f_{ij} = 2\left(\boldsymbol{d}_i \cdot \boldsymbol{d}_j + \boldsymbol{d} \cdot \boldsymbol{d}_{ij}\right) \quad \text{with } \bullet_i = \partial \bullet / \partial \alpha_i . \tag{10}$$

According to (8) the derivatives of the distance vector are obtained from the surface points derivatives

$$\begin{aligned} \boldsymbol{p}_i^{\beta} &= \frac{\partial \boldsymbol{p}^{\beta}}{\partial \phi_{\gamma}} \frac{\partial \phi_{\gamma}}{\partial c_k} \frac{\partial c_k}{\partial \alpha_i} \\ \boldsymbol{p}_{ij}^{\beta} &= \frac{\partial^2 \boldsymbol{p}^{\beta}}{\partial \phi_{\gamma} \, \partial \phi_{\delta}} \frac{\partial \phi_{\gamma}}{\partial c_k} \frac{\partial \phi_{\delta}}{\partial c_l} \frac{\partial c_k}{\partial \alpha_i} \frac{\partial c_l}{\partial \alpha_j} + \\ & \quad \frac{\partial \boldsymbol{p}^{\beta}}{\partial \phi_{\gamma}} \left( \frac{\partial^2 \phi_{\gamma}}{\partial c_k \, \partial c_l} \frac{\partial c_k}{\partial \alpha_i} \frac{\partial c_l}{\partial \alpha_j} + \frac{\partial \phi_{\gamma}}{\partial c_k} \frac{\partial^2 c_k}{\partial \alpha_i \, \partial \alpha_j} \right) . \end{aligned} \tag{11}$$

Herein repeated Greek indices denote a summation from 1 to 2 and repeated Latin indices denote a summation from 1 to 3. The single partial derivatives in (11) are derived from (2), (4), (6) and (7). Care has to be taken because some of the second derivatives $\partial^2 \boldsymbol{p}^{\beta} / \left(\partial \phi_{\gamma} \, \partial \phi_{\delta}\right)$ become indeterminate at points where $\sin \phi_{\gamma} = 0$ or $\cos \phi_{\gamma} = 0$. Furthermore, some of the derivatives $\partial \phi_{\gamma} / \partial c_k$ become indeterminate at points where one or more of the local transforms of the

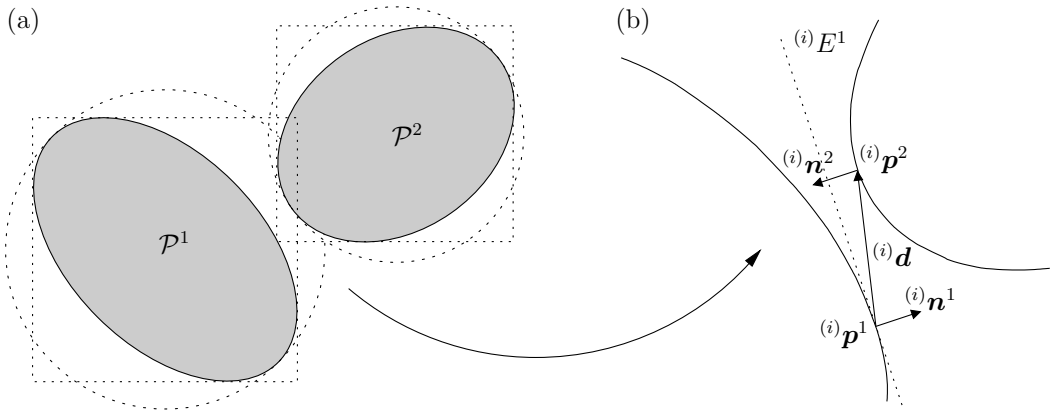


Fig. 3. (a) Two adjacent particles $\mathcal{P}^1$ and $\mathcal{P}^2$ with intersecting spherical and cuboid bounding boxes. (b) Contact points, normals and distance vector after $i$ iterations. ${}^{(i)}E^1$ is the tangent plane to $\mathcal{P}^1$ at ${}^{(i)}\boldsymbol{p}^1$.

$c_k$'s become zero. In these cases the points are slightly shifted to compute the gradient and Hessian of $f$. Start values for the direction angles can be drawn from the last time step of the DEM simulation if the particle pair has already been considered. Otherwise the direction of the vector connecting the particle centers is used as initial guess for the contact direction leading to ${}^{(0)}\alpha_i = 0$, compare (6).

The advantage of this approach is that in the case of non-penetrating particles a penetration can be ruled out before the iterative process converges to the exact contact direction, see Fig. 3. In part (a) two adjacent particles are depicted whose bounding boxes intersect. Hence, in a DEM simulation this particle pair will have to be checked for a penetration. Part (b) shows the contact points, normals and the distance vector after $i$ iterations. At this point of the iterative process a penetration can be ruled out, because it is

$$ {}^{(i)}\boldsymbol{n}^1 \cdot {}^{(i)}\boldsymbol{d} > 0 \;\Leftrightarrow\; {}^{(i)}\boldsymbol{c} \cdot {}^{(i)}\boldsymbol{d} > 0\,. \tag{12} $$

Because of $(5)_1$, $(5)_2$ and (12) ${}^{(i)}\boldsymbol{p}^2$ is the closest point of $\mathcal{P}^2$ to the tangent plane ${}^{(i)}E^1$ with a distance unequal zero. Therefore, ${}^{(i)}E^1$ separates $\mathcal{P}^1$ and $\mathcal{P}^2$ and a penetration can be ruled out. The criteria (12) is checked for every contact direction ${}^{(i)}\boldsymbol{c}$ in the course of the iterative process. If it is fulfilled the algorithm stops. Since only one additional vector product is required this leads to a significant speed up of the contact detection process.

In the case of a penetration of $\mathcal{P}^1$ and $\mathcal{P}^2$ the algorithm converges to a minimum of $f$. To ensure that this minimum is the global minimum two conditions have to be checked. First, $(5)_3$ has to be fulfilled. Under the assumption of a small penetration distance $(5)_3$ can only be fulfilled by a local minimum if the corresponding contact points $\boldsymbol{p}^1$ and $\boldsymbol{p}^2$ lie outside $\mathcal{P}^2$ and $\mathcal{P}^1$, see Fig. 4. Hence, the second condition that has to be checked is that $\boldsymbol{p}^1 \in \mathcal{P}^2$ and $\boldsymbol{p}^2 \in \mathcal{P}^1$, which can be done using the inside-outside functions of the particles. If convergence to a local minimum is detected a combination of a random-

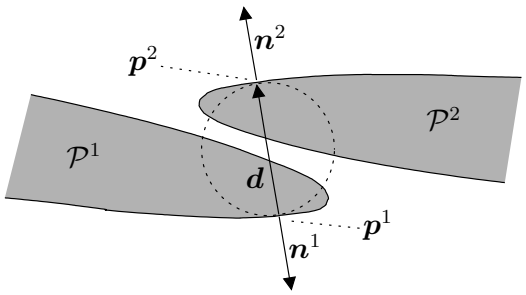


Fig. 4. Two adjacent particles $\mathcal{P}^1$ and $\mathcal{P}^2$ with contact points, normals and distance vector corresponding to a local minimum of $f$. The dotted circle indicates that $\boldsymbol{d}$ has locally minimum length.

search method and the NELDER-MEAD simplex algorithm (Lagarias et al., 1998) is applied to generate a new start point. This process is repeated until the global minimum of $f$ is found.

## Validation

The contact detection algorithm was validated by means of two test series with randomly generated particle pairs. In the first test series all particle pairs have a real distance while in the second series there is always a small penetration. For all tests the superellipsoid radius parameters $r_i$ were chosen randomly and equally distributed from the interval $(0.5, 3.0)$ yielding a maximum particle aspect ratio of 6. The squareness parameters $\epsilon_i$ were chosen from the three intervals listed below.

| interval # | 1 | 2 | 3 |
|---|---|---|---|
| $\epsilon_{\min}$ | 1 | 0.7 | 0.3 |
| $\epsilon_{\max}$ | 1 | 1.3 | 1.7 |

The positions and orientations of the particles were generated according to the following scheme: The first particle center is set to the origin $\boldsymbol{s}^1 = \boldsymbol{0}$ and it's rotation tensor is set to the unit tensor $\boldsymbol{T}^1 = \boldsymbol{E}$. Next, a random contact direction $\boldsymbol{c}$ is generated from which the surface parameters $\phi_i^1$ of the contact point $\boldsymbol{p}^1$ can be determined using (4) and (7). A random rotation tensor $\boldsymbol{T}^2$ is generated and the distance $d$ of the particles is chosen. Finally $\boldsymbol{p}^2$ is derived from $\boldsymbol{p}^1$, $d$ and $\boldsymbol{c}$ and $\boldsymbol{s}^2$ is calculated from $\boldsymbol{p}^2$ and $\boldsymbol{T}^2$ with the help of (2) and (7).
For both test series $10^6$ particle pairs were generated for each squareness parameter interval. The direction of the vector connecting the particle centers was used as initial guess for the contact direction. The distance of the particles for the first test series was chosen randomly and equally distributed from the

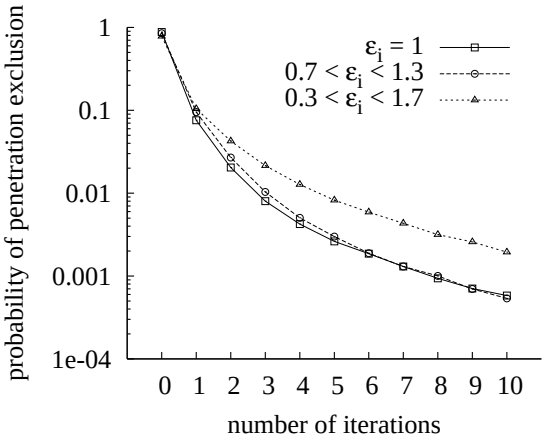


Fig. 5. First test series: Probability of a penetration exclusion vs. the number of iterations.

interval $(0, 0.25)$. The number of iterations needed to rule out a penetration was recorded. The probability of a penetration exclusion after $i$ iterations, which is the number of trials where a penetration was ruled out after $i$ iterations divided by the overall number of trials, is plotted against $i$ in Fig. 5. The probability of a penetration exclusion after 0 iterations is 78.2% for the squareness parameter interval 3, 85.2% for interval 2 and 88.1% for interval 1. In this case the initial guess for the contact direction is good enough to rule out a penetration, so no gradient or Hessian has to be computed. The probability that 5 or more iterations are needed is 3.7% for interval 3, 1.1% for interval 2 and 1.1% for interval 1. The number of trials where a penetration could not be excluded within 50 iterations is 456 for interval 3, 24 for interval 2 and 28 for interval 1. In these cases at most 3 new start points had to be generated until a penetration could be excluded.

In the second test series the penetration distance was chosen randomly and equally distributed from the interval $(0, 1.75 \cdot 10^{-3})$. The algorithm stopped when it reached an accuracy of $\|\text{grad} f\| < 10^{-6}$ and the number of iterations performed was recorded. The results are plotted in Fig. 6. For each squareness parameter interval convergence is most likely reached after about 2 - 10 iterations. The probability that 20 or more iterations are needed is 4.5% for interval 3, 0.4% for interval 2 and 0.4% for interval 1. The number of trials where the algorithm converged to a local minimum or did not converge within 50 iterations is 9219 for interval 3, 198 for interval 2 and 193 for interval 1. Here at most 15 new start points had to be generated for interval 3 and 2 for interval 2 and 1.

Finally, the accuracy of the algorithm was analyzed in terms of the relative error of the computed penetration distance $\tilde{d}$, the distance of the computed and the exact contact points $\tilde{\boldsymbol{p}}^i$ and $\boldsymbol{p}^i$ and the angle between the computed and exact contact direction $\tilde{\boldsymbol{c}}$ and $\boldsymbol{c}$. The average values for each squareness parameter interval are listed in Table 1.

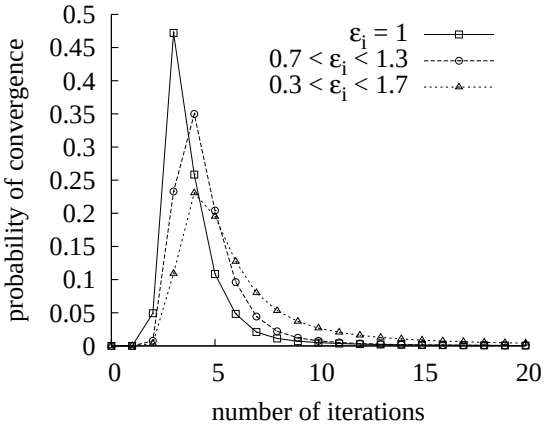


Fig. 6. Second test series: Probability to reach convergence vs. the number of iterations.

| interval # | $\lvert\tilde{d}-d\rvert/d$ | $\lVert\tilde{\boldsymbol{p}}^i-\boldsymbol{p}^i\rVert$ | $\arccos(\tilde{\boldsymbol{c}}\cdot\boldsymbol{c})$ [°] |
|---|---|---|---|
| 1 | $2.34\cdot10^{-6}$ | $4.34\cdot10^{-8}$ | $4.21\cdot10^{-3}$ |
| 2 | $2.40\cdot10^{-6}$ | $4.40\cdot10^{-8}$ | $5.05\cdot10^{-3}$ |
| 3 | $3.21\cdot10^{-5}$ | $3.72\cdot10^{-7}$ | $1.82\cdot10^{-2}$ |

Table 1
Average errors of contact detection algorithm results.

## Conclusion

A contact detection algorithm is introduced that is applicable to convex continuous particles, which offer an explicit relationship between contact normals and surface points. The main characteristic of the algorithm is that it searches for the contact direction instead of the contact points. This, in combination with the convex particle shape, offers the possibility of a penetration exclusion before final convergence is reached. Numerical tests showed that a fast penetration exclusion is very probable yielding a high efficiency of the algorithm when applied to non-penetrating particle pairs. In the case of a penetration the algorithm most likely converges in less than ten iterations yielding a high accuracy in terms of the penetration distance, contact points and contact direction. Therefore, the algorithm is expected to show good performance when applied to DEM simulations of convex continuous particles.

## References

A. H. Barr. Superquadrics and angle-preserving transformations. *IEEE Computer Graphics and Applications*, 1(1):11–23, 1981.

P.W. Cleary, N. Stokes, and J. Hurley. Efficient collision detection for three

dimensional super-ellipsoidal particles. Proceedings of 8th International Computational Techniques and Applications Conference CTAC97, Adelaide, 1997.

C. Hogue. Shape representation and contact detection for discrete element simulations of arbitrary geometries. *Engineering Computations*, 15(3):374–390, 1998.

K. L. Johnson. *Contact Mechanics*. Cambridge University Press, 1985.

S. Johnson, J. R. Williams, and B. Cook. Contact resolution algorithm for an ellipsoid approximation for discrete element modeling. *Engineering Computations*, 21(2/3/4):215–234, 2004.

M. R. Kuhn. Smooth convex three-dimensional particle for the discrete-element method. *Journal of Engineering Mechanics*, 129(5):539–547, 2003.

J. C. Lagarias, J. A. Reeds, M. H. Wright, and P. E. Wright. Convergence properties of the nelder-mead simplex algorithm in low dimensions. *SIAM Journal on Optimization*, 9:112–147, 1998.

M. C. Lin and S. Gottschalk. Collision detection between geometric models: a survey. Proceedings of IMA Conference on Mathematics of Surfaces, 1998.

X. Lin and T.-T. Ng. Contact detection algorithms for three-dimensional ellipsoids in discrete element modelling. *International Journal for Numerical and Analytical Methods in Geomechanics*, 19(9):653–659, 1995.

H. Ouadfel and L. Rothenburg. An algorithm for detecting inter-ellipsoid contacts. *Computers and Geotechnics*, 24(4):245–263, 1999.

A. V. Potapov and C. S. Campbell. A fast model for the simulation of non-round particles. *Granular Matter*, 1(1):9–14, 1998.

E. Tijskens, J. De Baerdemaeker, and H. Ramon. Strategies for contact resolution of level surfaces. *Engineering Computations*, 21(2/3/4):137–150, 2004.

J. M. Ting, M. Khwaja, L. R. Meachum, and J. D. Rowell. An ellipse-based discrete element model for granular materials. *International Journal for Numerical and Analytical Methods in Geomechanics*, 17(9):603–623, 1993.

J. M. Ting, L. R. Meachum, and J. D. Rowell. Effect of particle shape on the strength and deformation mechanisms of ellipse-shaped granular assemblages. *Engineering Computations*, 12(2):99–108, 1995.

B. C. Vemuri, Y. Cao, and L. Chen. Fast collision detection algorithms with applications to particle flow. *Computer Graphics Forum*, 17(2):121–134, 1998.

C.-Y. Wang, C.-F. Wang, and J. Sheng. A packing generation scheme for the granular assemblies with 3d ellipsoidal particles. *International Journal for Numerical and Analytical Methods in Geomechanics*, 23(8):815–828, 1999.

J. R. Williams and R. O'Connor. A linear complexity intersection algorithm for discrete element simulation of arbitrary geometries. *Engineering Computations*, 12(2):185–201, 1995.

J. R. Williams and A. P. Pentland. Superquadrics and modal dynamics for discrete elements in interactive design. *Engineering Computations*, 9(2): 115–127, 1992.